

A Piecewise Linear Model for Passive Intermodulation Distortion

Khaled M. Gharaibeh

Department of Telecommunications Engineering, Hijjawi Faculty for Engineering Technology, Yarmouk University, Irbid, Jordan

Email: kmgharai@yu.edu.jo (K.M.G.)

Abstract—Passive Intermodulation (PIM) distortion which results from passive components such as antennas, connectors, etc. poses significant challenges in wireless communications by limiting cell coverage and data rates. In Carrier Aggregated (CA) Long-Term Evolution (LTE) system, PIM is manifested as self-interference when intermodulation products of the transmitted signal leak to the receiver. The primary goal of this paper is to develop a new behavioral model for passive nonlinearities enabling PIM distortion in LTE systems to be predicted. The analysis employs a Threshold-Decomposition-based Piecewise Linear (TD-PWL) model to represent a passive nonlinearity and predict PIM in CA-LTE system. Simulation results show that the proposed model accurately predicts PIM and highlight its superior numerical stability and accuracy over polynomial-based models. These results position the PWL model as a promising choice in the design of PIM cancellation schemes.

Keywords—passive intermodulation, piecewise linear model, Long Term Evolution (LTE), behavioral models, Threshold decomposition

I. INTRODUCTION

Modern mobile communication systems require large link budgets due to the need for larger coverage areas and capacity. The large link budgets mean that high linearity requirements in the transmit signal path are required as nonlinearity results in degradation of overall system performance. Nonlinear distortion can result from nonlinear active circuits such as mixers or amplifiers, or from passive devices such as filters, antennas, connectors and transmission lines. Active nonlinear distortion is usually manifested as intermodulation products that have significant power levels and hence, can easily be characterized and then removed using filtering or linearization techniques. Unfortunately, Passive Intermodulation (PIM) distortion results in weak intermodulation products and may only grow to significant levels as passive components age or corrode. Hence, PIM is very difficult to diagnose, troubleshoot and model [1].

In general, there are two sources of PIM. The first is related to current flowing in junctions with different materials such as metal-to metal or metal to insulator contacts. The second is related to nonlinear passive

materials where the current response of the material to an applied voltage has nonlinear characteristics. The first category includes loose or oxidized joints while the second includes conductive properties of the material [2].

Although the PIM phenomena existed in early cellular systems (1G and 2G), it has become more significant with modern cellular systems such as 3 to 5G systems [3]. This is because the increased density and diversity of base station towers which utilize antenna sharing made PIM more significant. In such configurations, passive components generate significant amounts of PIM, especially if these are poorly installed or affected by weather.

PIM is notably evident in modern wideband systems that employ multichannel transmission such as CA-LTE systems. In such system, the transmitted signal which consists of aggregated carriers, is subject to passive nonlinearities in the duplexing stage. The passive nonlinearity produces intermodulation products which may lie in the receive band. If these IM components leak to the receiver due to imperfect duplexing, they can cause significant interference at the receiver. This interference being substantially stronger than the desired weak received signal may cause complete blocking of the received or limit the capacity of the communication system and compromise its throughput [4]. Experimental studies showed that the download speed may drop by 20% when PIM levels increase by 20 dB (for example from -125 dBm to -105 dBm) [6].

An illustration of this phenomenon is demonstrated in Fig. 1, which shows a diagram for PIM generation process in CA system. The transmitted signal which consists of CA channels is subjected to a passive nonlinearity represented by the PIM source. A simple example of this scenario is PIM interference in an CA-LTE base station system as shown in Fig. 2. The transmit band of LTE systems ranges from 1930 MHz to 1990 MHz while the receive band ranges from 1850 MHz to 1910 MHz. If the transmitted signal consists of two signals centered at $f_1=1940$ MHz and $f_2=1980$ MHz, then their third-order intermodulation products generated by the passive nonlinearity will be centered at $2f_2 - f_1=1900$ MHz which will fall into the receive band [1]. If these intermodulation products leak to the receiver through the duplexer, significant interference

will be introduced which leads to significant receiver desensitization [1].

The obvious solution to the receiver desensitization problem in such a system is to reduce the transmit power or relax the receiver sensitivity, however, this will severely compromise the uplink coverage [4]. A straightforward alternative to this is using high-quality materials, however, using high quality materials is usually costly and hence, unreliable from a quality assurance standpoint of the manufacturing process. Other solutions include developing guidelines for minimization of PIM such as minimizing loose contacts, minimizing thermal variations, minimizing cable lengths, etc. but these usually result in increased cost and power requirements [7].

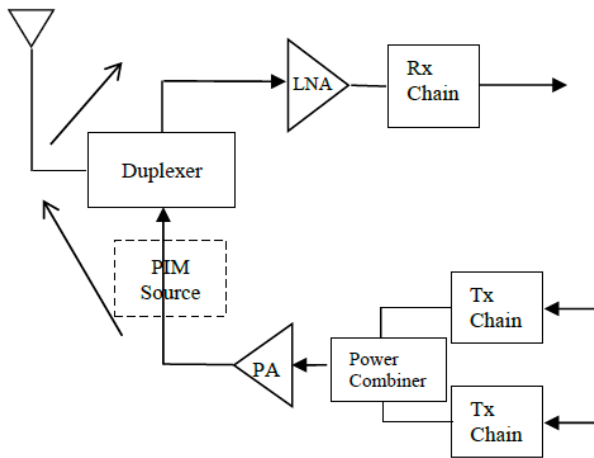


Fig. 1. PIM generation in a wireless transceiver.

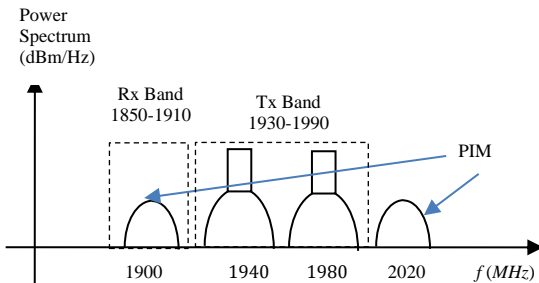


Fig. 2. Output spectrum of a passive nonlinearity for a two CA channels input.

The alternative to the above measures is to use PIM cancellation schemes where PIM components are cancelled either in the analog or digital domains [8]. PIM cancellation is based on developing a nonlinear model for the passive nonlinearity. The model is then used to reconstruct a PIM signal from the input signals at the transmitter which can then be used to cancel the PIM components at the receiver.

Nonlinear models are based on either physical or behavioral models. Physical models are usually very sophisticated and not easy to validate if the physical mechanisms are not fully understood [9]. This is because the PIM phenomena seems to result from multiple physical nonlinear mechanisms such as thermal, mechanical or charge trapping. Identifying and discriminating these mechanisms is difficult, thereby complicating the

modeling process [2]. In contrast, behavioral models have been more attractive as they are usually based on fitting measured characteristics to simple mathematical models inspired by the physical phenomena.

Significant research has been undertaken on developing behavioral models for passive nonlinearities. The most popular models have been the polynomial-based models. In [10], it was shown using measurements that the polynomial model can adequately describe the frequency mixing process that results from passive nonlinearities in a transmission line. However, as was shown in [11], the polynomial model is not well suited for modelling PIM-producing components such as coaxial connections. The main reason for that is that the slope of PIM characteristics is not constant with respect to the input power which renders the polynomial model incapable for addressing this phenomenon [12]. Furthermore, the polynomial-based models lack numerical stability especially with hard nonlinearities as will be seen in the next sections.

Zhang *et al.* [13] presented a composite exponential model to characterize PIM which considers the correlation between the PIM products and their dependence on carrier power. They validated the model using measurements on a microwave filter. Zhang *et al.* [14] used segmented polynomial model to accurately model PIM. The model, which was verified by measurements, captured the dependence of PIM on carrier power and was shown to require a smaller number of parameters than the traditional polynomial model. Kozlov *et al.* [15] developed a memoryless nonlinear polynomial model for prediction of high-order intermodulation distortion in multi-carrier systems. The model was based on extraction of parameters from two tone measurements on a microstrip transmission line with distributed nonlinearity. They showed that models based on two-tone measurements tend to underestimate crossband interference when the input to the model consists of two modulated signals. Conversely, in the case of three modulated signals, it was shown that these models tend to overestimate PIM [16].

In essence, behavioral models consider the dependence of PIM on power, frequency bandwidth, signal modulation temperature and perhaps other factors. Nevertheless, they are complicated by the difficulty of validating them in specific situations. Furthermore, the accuracy of these behavioral models depends on the ability to identify the physical mechanisms by which PIM occurs [17].

This paper aims to develop a new behavioral model for predicting PIM with the objective of enhancing the accuracy of available models. A PWL model based on the concept of TD is proposed to model a passive nonlinearity and to accurately predict PIM. The model is based on segmentation of the nonlinear characteristics which results in a more numerically stable model with a high dynamic range than the traditional polynomial model. The model is used to predict PIM in a carrier aggregated LTE system where it is shown that it accurately predicts PIM components which results from a passive nonlinearity in a CA-LTE system.

II. MODELING OF A PIM SOURCE

The PIM source in Fig. 1 refers to passive Radio Frequency (RF) and microwave components such as coaxial connectors in the duplexing stage. These components exhibit nonlinear characteristics due to their low-quality commercial materials and fabrication flaws. The nonlinear characteristics of such passive devices usually produce intermodulation power that deviate from the conventional 3dB/dB slopes of intermodulation power produced by active nonlinearities. This phenomenon was studied in [18] where PIM generated by electro-thermally induced nonlinearities of a resistive element was analyzed. The analysis showed that third order intermodulation products of nonlinearities that result from decreasing-resistance produce less than 3 dB/dB regrowth, while those of increasing-resistance produce greater than 3 dB/dB regrowth.

The deviation of passive nonlinear characteristics from the 3dB/dB regrowth means that traditional nonlinear models for active devices (such as the Rapp model and the Saleh model) cannot be used to model passive nonlinearities [19]. Therefore, an often-utilized model for such passive nonlinearity is the hyperbolic tangent model which is given by the following I/V characteristics:

$$I(t) = g_0[1 + k_1 \tanh(k_2 V(t))] \quad (1)$$

where g_0 , k_1 , k_2 are model parameters which can be determined from the material properties of the PIM source. Fig. 3 shows the I/V characteristics of the hyperbolic tangent model in Eq. (1).

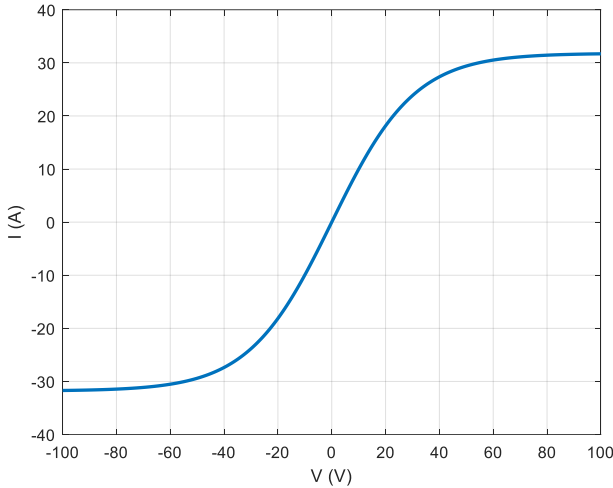


Fig. 3. Nonlinear characteristics generated using the hyperbolic tangent model in Eq. (1).

The hyperbolic tangent model was shown in [19] to follow measured PIM characteristics of coaxial connector over an input power range of 30–70 dB by the proper selection of the two independent parameters k_1 and k_2 . Moreover, this model is deemed suitable for modeling a passive nonlinearity for many reasons. Firstly, the magnetization model used to characterize nonlinearity in a coaxial structure follow the hyperbolic tangent characteristics [20, 21]. Secondly, a passive nonlinearity

which result from multiple sources (such as multiple coaxial connectors) follows a hyperbolic tangent characteristic as demonstrated in [11]. Finally, the hyperbolic tangent function has an intriguing property that its derivative is also a hyperbolic tangent function. As a result, its second derivative becomes proportional to the linear combination of the first order and the third order of the input which are direct measures of the nonlinear behavior [22].

In the following sections, the PIM source in Fig. 1 is assumed to follow the hyperbolic tangent characteristics in Eq. (1). Subsequently, a TD-PWL behavioral model is developed by fitting a TD-PWL model to the hyperbolic tangent characteristics. The behavioral model is then used to predict PIM power in accordance with the scenario shown in Fig. 2.

III. THE TD-PWL BEHAVIORAL MODEL

A. Model Development

In this section, we propose using a PWL model to model a passive nonlinearity that follows hyperbolic tangent characteristics. The rationale for using the PWL approximation for modeling passive nonlinearities stems from the fact that the PWL model is suitable for approximating hyperbolic tangent characteristics as shown in [23].

The proposed TD-PWL model represents the passive nonlinear characteristics as linear combination of the segmented input as

$$y(t) = F(x(t)) = \sum_{i=1}^K a_i X_i(t) \quad (2)$$

Here $F(\cdot)$ represents the passive nonlinearity, $\{a_i\}$ are the model coefficients and $X_i(t)$ represents the i -th segment of the input signal which are obtained using the TD operator. The TD operator is simply a soft limiter operator of the form [24]:

$$X_i(t) = \begin{cases} \lambda_{i+1} - \lambda_i & |x(t)| > \lambda_{i+1} \\ x(t) - \lambda_i & \lambda_i \leq |x(t)| \leq \lambda_{i+1} \\ 0 & |x(t)| < \lambda_i \end{cases} \quad (3)$$

where, $\{\lambda_i\}$ is a set of thresholds. The TD-PWL model output can be written in matrix form as

$$\mathbf{Y} = \Psi_X \mathbf{a} \quad (4)$$

where, $\mathbf{a} = [a_1 \ a_2 \ \dots \ a_K]^T$ is a $K \times 1$ vector which represents the coefficients of the PWL model, \mathbf{Y} is a $M \times 1$ vector which represents the output signal and Ψ_X is a $M \times K$ matrix whose columns are the decomposed segments of the input:

$$\Psi_X = [X_1(t) \ X_2(t) \ \dots \ X_K(t)] \quad (5)$$

The model coefficients can then be extracted through linear regression using Least Squares (LS) optimization as

$$\mathbf{a} = \Psi_X^+ \mathbf{Y} \quad (6)$$

where \mathbf{Y} is the measured output vector and $\Psi_X^+ = (\Psi_X^H \Psi_X)^{-1} \Psi_X$ is the Moore-Penrose pseudo inverse of Ψ_X and H indicates the Hermitian transpose.

Fig. 4 shows a PWL fit to the nonlinear characteristics of the hyperbolic tangent function for $K=3$ and $K=5$. By visual inspection, it is clear that the PWL model provides a good fit to the hyperbolic tangent characteristics for $K \geq 5$.

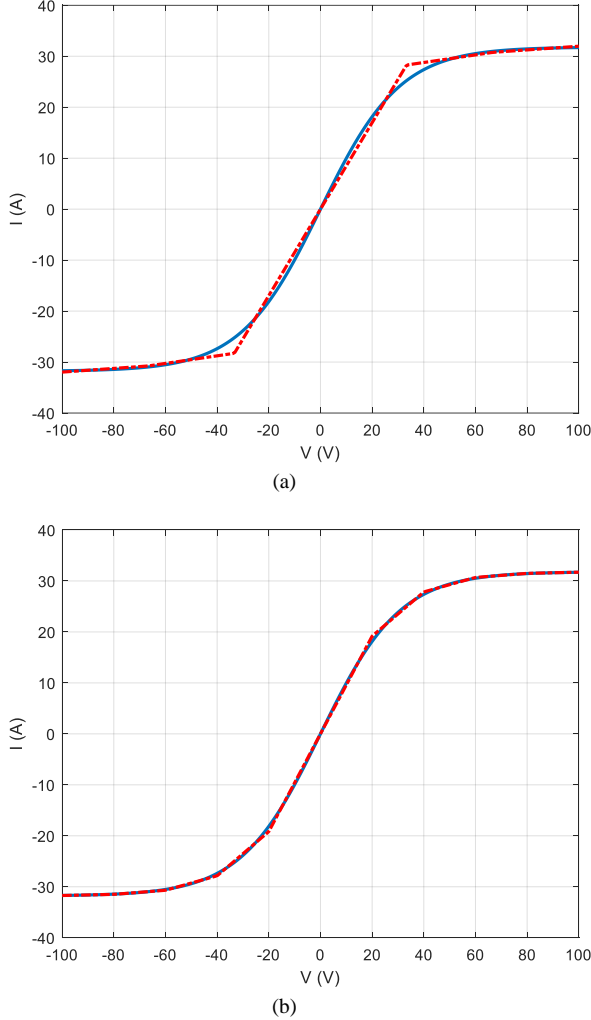


Fig. 4. TD-PWL fit to the hyperbolic tangent nonlinear characteristics: Solid: hyperbolic tangent model and dashed: PWL model; (a) $K=3$ and (b) $K=5$.

B. Remarks

The correlation between the columns of the regressor matrix is characterized by the condition number of the matrix [1]. High correlation (and hence, a high condition number) of the regressor matrix means that the model output will exhibit large deviation in the output for small variations in the input. On the other hand, a high condition number of the regressor matrix results in the inability of the model to predict nonlinear distortion when the input consists of complex signals that have high Peak to Average Ratios (PAR) such as digitally modulated signals of finite bandwidth.

The TD-PWL model is essentially a linear combination of threshold decomposed segments of the input signal where the continuity at the boundaries of the segments is ensured by the properties of the TD operator. This results in a regression matrix Ψ_X with low correlation among its

columns regardless of the model order. Hence, the condition number of the matrix does not increase significantly with increasing the model order. This gives the PWL an advantage over the polynomial model which has a regressor matrix in the form of a Vandermonde matrix which is given by [12]:

$$\Phi_X = \begin{bmatrix} 1 & x & x^2 & \dots & x^n \\ 1 & x & x^2 & \dots & x^n \\ \vdots & \vdots & \vdots & \dots & \vdots \\ 1 & x & x^2 & \dots & x^n \end{bmatrix} \quad (7)$$

Note that the Vandermonde matrix consists of highly correlated monomials indicating high condition number, especially if the model order is high.

Consequently, the PWL model offers an advantage over the polynomial model when the nonlinearity is hard as hard nonlinearities require a high model order to achieve acceptable modeling accuracy. Furthermore, the low condition number of the regressor matrix of the PWL model will also make it more suited than the polynomial model for predicting nonlinear distortion when the input signal has high PAR.

Fig. 5 depicts the Mean Squared Error (MSE) between the behavioral model output ($P_{o_{model}}$) and the hyperbolic tangent characteristics ($P_{o_{tanh}}$) versus the number of coefficients. The MSE is defined as:

$$MSE = |P_{o_{model}} - P_{o_{tanh}}|^2 \quad (8)$$

The plot reveals that the MSE of the polynomial model fluctuates with varying coefficient numbers, indicating no fidelity improvement with increased model order. Conversely, the PWL model displays a smooth decrease in MSE with increasing the number of model coefficients, suggesting its suitability for modeling hard nonlinearities that necessitate higher orders [25].

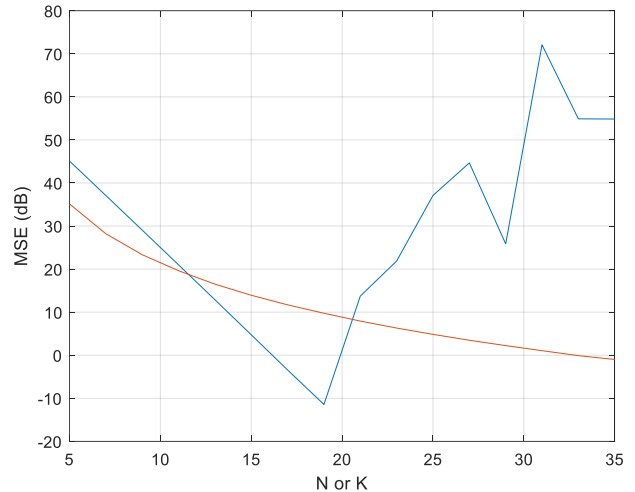


Fig. 5. MSE vs. number of coefficients (N or K): (red): PWL and (blue): polynomial model.

Additionally, prior research demonstrates the inadequacy of the polynomial model in modeling PIM-producing components like coaxial connections [11]. Polynomial models establish an n -th order proportion between input power and the n -th intermodulation product,

which conflicts with measured PIM characteristics which typically exhibit slopes smaller than ‘n’ [26]. Though higher-order polynomials can address this issue, they lead to an unstable model, emphasizing the suitability of the PWL model’s for modeling passive nonlinearities.

C. PIM Cancellation Using the PWL Model

The PWL model can be incorporated into a PIM cancellation loop within a CA-LTE base station, as shown in Fig. 6, [26, 27]. For simplicity, the active nonlinearities of the LNA and the PA are neglected in this model. In this system, the transmitted signal consists of the sum of two aggregated carriers $x_1(t)$ and $x_2(t)$ centered at f_1 and f_2 . Assuming offline parameter estimation, where the uplink received signal (denoted by $r_0(t)$) is absent, the available signal at the receiver consists of only the leaked signal from the transmitter $x(t)$ after being processed by the PIM source. Therefore:

$$r(t) = F(x(t)) \quad (9)$$

where, $F(\cdot)$ represents the passive nonlinearity. The PIM estimation block produces the model coefficients by comparing the transmitted signal to the output of the passive nonlinearity at the receiver. The model coefficients can be developed using Eq. (6) where the vector \mathbf{Y} consists of the samples of $r(t)$ and Ψ_X consists of threshold-decomposed segments of the transmitted signal $x(t)$. After training the system, the model coefficients \mathbf{a} produced by the PIM estimation block can be used to produce a cancelling signal as

$$z_c(t) = \text{BPF}\{\sum_{i=1}^K a_i X_i(t)\} \quad (10)$$

where BPF indicates a bandpass filter centered at the PIM frequencies. The cancelling signal is then fed to the receiver at online operation to cancel the PIM interference. In this case, the received signal is

$$r(t) = r_0(t) + F(x(t)) \quad (11)$$

And hence, the signal at the receiver chain is

$$r_c(t) = r(t) - z_c(t) = r_0(t) \quad (12)$$

which consists of only the uplink received signal without PIM.

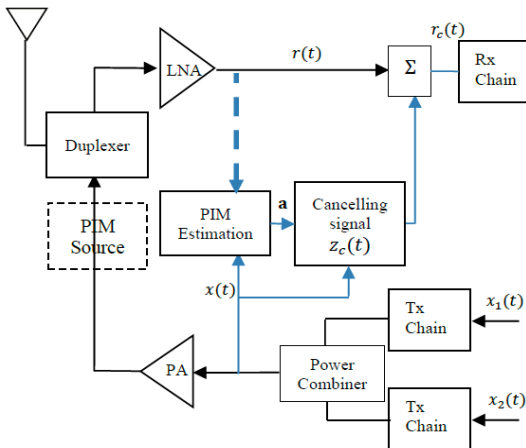


Fig. 6. PIM cancellation scheme in a CA-LTE system.

The PIM cancellation scheme can be implemented adaptively where PIM cancelation is done continuously during online operation of the radio transceiver [28].

IV. SIMULATION RESULTS

In this section, simulation results of the above concepts are presented and discussed. The objective of the simulations is to show that the PWL model is well suited for modeling PIM in CA-LTE systems and that it outperforms the polynomial model.

The passive nonlinearity was generated using the hyperbolic tangent characteristics with parameters $k_1 = 6 \times 10^{-4}$, $k_2 = 3 \times 10^{-2}$ and $g_0=1$. Then a polynomial model and a TD-PWL model were developed for these nonlinear characteristics using LS optimization. Table I shows the coefficients of both models for $N=13$ and $K=13$.

The capability of the PWL model to predict PIM in an LTE system is defined as the input power range of an OFDM signal for which the model provides a good estimate of PIM distortion. For this purpose, the two models (PWL and polynomial) were fed with two CA OFDM signal with 20 MHz bandwidth and a frequency separation of 120 MHz. The power spectral density (PSD) of the output of the nonlinear model was computed using the periodogram of the output of the model is expressed as [29]:

$$p_{x_w, M}(\omega) = \frac{1}{M} \left| \sum_{n=0}^{M-1} y_w(n) e^{-j\omega n} \right|^2 \quad (13)$$

where $y_w(n) = y(n)w(n)$ is the windowed signal and $w(n)$ is the window function and M is the signal size. A Hanning window was used in the simulations as it provides better prediction capability of PIM as was shown in [29].

Fig. 7 shows the Power Spectral Density (PSD) at the output of a PIM source characterized by the hyperbolic tangent model when the input consists of two-OFDM signals. The figure shows the PIM components that appear at the intermodulation frequencies.

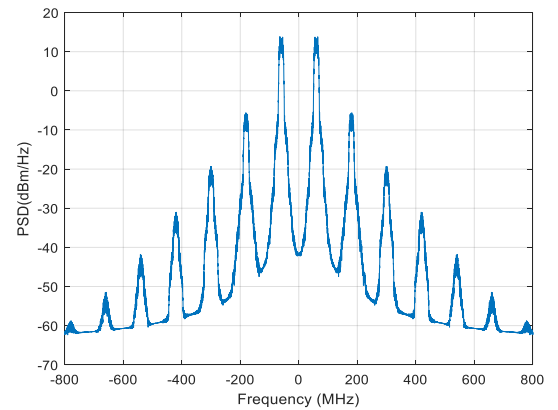


Fig. 7. Power spectral density at the output of the PIM source (modeled by a hyperbolic tangent characteristics) for an input that consists of two-OFDM signals.

In a wide band system, the instability of the polynomial model is manifested as overestimation of the PIM power when the transmitted signal consists of two OFDM signals as shown in Fig. 8 (a). The figure shows that the polynomial model fails to predict PIM and produces an output that overestimates the PIM components. The reason

for this is that the OFDM signals have a high PAR which tend to drive the model beyond the power limit on which the model was extracted. In contrast, Fig. 8(b) shows that the PWL model provides a stable estimation of the PIM products even when the model is driven beyond its input power limit.

TABLE I. PWL AND POLYNOMIAL MODEL COEFFICIENTS FOR THE HYPERBOLIC TANGENT NONLINEARITY

PWL Coefficients		Polynomial Model Coefficients	
a_1	1.45563	b_1	1.0303
a_2	1.43757	b_3	-3.6048×10^{-04}
a_3	1.40262	b_5	1.4993×10^{-07}
a_4	1.35217	b_7	-4.4793×10^{-11}
a_5	1.28853	b_9	-1.1546×10^{-13}
a_6	1.21463	b_{11}	6.4532×10^{-16}
a_7	1.13305	b_{13}	-1.7754×10^{-18}
a_8	1.04682	—	—
a_9	0.95845	—	—
a_{10}	0.87069	—	—
a_{11}	0.78492	—	—
a_{12}	0.70286	—	—
a_{13}	0.62436	—	—

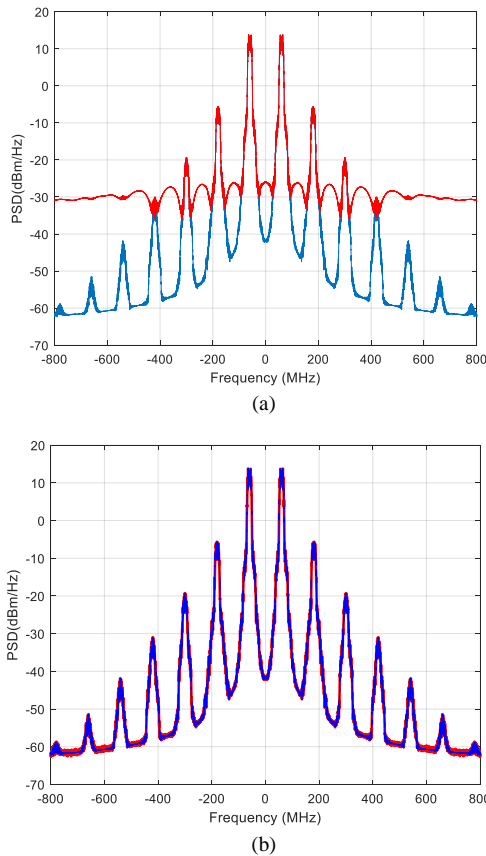


Fig. 8. The PSD at the output of a passive nonlinearity; (hyperbolic tangent characteristics) (solid); and behavioural model (dashed)); (a) polynomial model and (b) the PWL model.

Figs. 9 (a) and (b) show the power of the PIM components (3^{rd} to 7^{th} order products) predicted by both model vs. the input power. It is clear that the PWL model provides excellent match to the nonlinear output of the passive nonlinearity over the full range of the input power

(30 dB in this case). Conversely, the polynomial model can only model the passive nonlinearity over half the range of the input power only (about 18 dB). These results indicate that the PWL model is more efficient than polynomial-base models with regards to model stability and accuracy as well as low complexity given the small number of coefficients needed to model a passive nonlinearity.

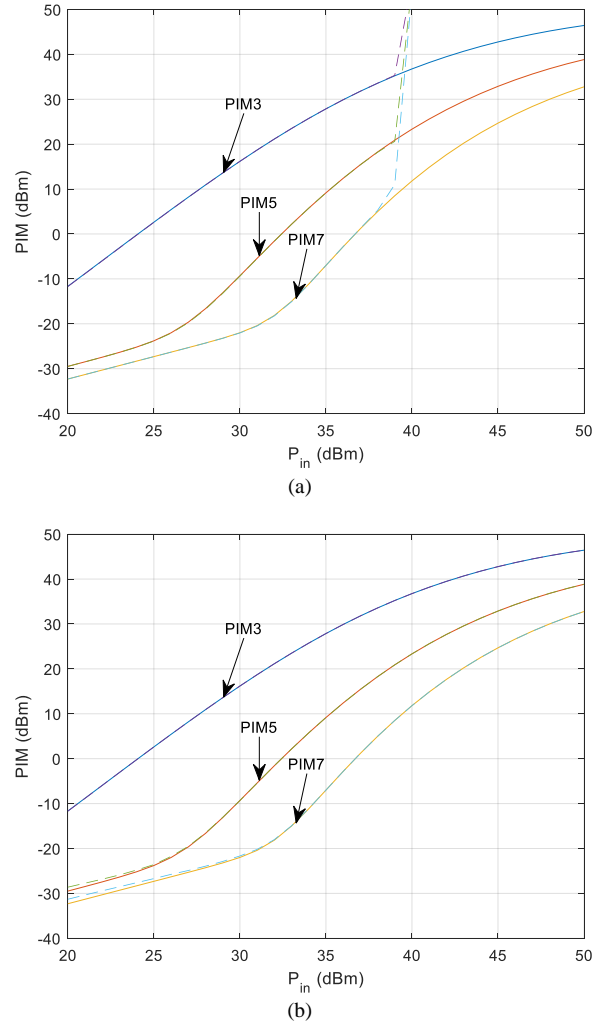


Fig. 9. PIM power vs. input power (hyperbolic tangent characteristics) (solid); and behavioural model (dashed)); (a): Polynomial model with $N=15$ and (b) PWL model with $K=15$.

V. CONCLUSION

A new approach for behavioral modeling PIM in wireless communication systems has been presented. The model is based on TD-PWL approximation of a passive nonlinearity. The proposed TD-PWL model was used to fit the passive nonlinearity characteristics represented by a hyperbolic tangent I/V characteristic which are commonly used to model passive nonlinearities. It has been shown that the TD-PWL is more numerically stable and is more economical in terms of the number of parameters than polynomial models, especially for hard nonlinearities which require high model orders. Given the stability and numerical effectiveness of the model, it has been shown that it can efficiently be used to predict PIM as well as to design efficient PIM cancellation schemes in CA-LTE

systems. The proposed model was verified by simulations where it has been shown that PWL model is more effective for modeling PIM in CA-LTE system than the traditional polynomial models in terms of modeling accuracy. The model can be extended to account for memory effects of passive nonlinearities but this is left for future research.

CONFLICT OF INTEREST

The author declares no conflict of interest.

REFERENCES

- [1] F. Kearney and S. Chen, "Passive Intermodulation (PIM) Effects in base stations: Understanding the challenges and solutions," *Analogdialogue*, p. 25, 2017.
- [2] Z. Cai, L. Liu, F. D. Paulis, and Y. Qi, "Passive intermodulation measurement: Challenges and solutions," *Engineering*, vol. 14, pp. 181–191.
- [3] L. Tong, Z. Pei, Z. Yanyun, and M. Dexiang, "The analysis of intermodulation interference for coexistence of different systems including 2G/3G/4G," in *Proc. 2014 URSI General Assembly and Scientific Symposium (URSI GASS)*, 2014, pp. 1–4.
- [4] A. Shitvov, A. Schuchinsky, and D. Kozlov, "Communication nonlinearities techniques for analysis of passive intermodulation," in *Proc. 6th International Workshop on Multipactor, Corona and Passive Intermodulation MULCOPIM*, vol. 6, 2014.
- [5] J. Jokinen, "Passive intermodulation in high-power radio transceivers," Master's Thesis, 2016.
- [6] Passive Intermodulation (PIM), Anritsu America. [Online]. Available: <https://www.anritsu.com>.
- [7] P. L. Lui, "Passive intermodulation interference in communication systems," *Electronics and Communication Engineering Journal*, vol. 2, no. 3, pp. 109–118, 1999.
- [8] X. Miao and L. Tian, "Digital cancellation scheme and hardware implementation for high-order passive intermodulation interference based on hammerstein model," *China Communications*, vol. 16, no. 9, pp. 165–176, 2019.
- [9] J. R. Wilkerson *et al.*, "Passive intermodulation distortion in antennas," *IEEE Transactions on Antennas and Propagation*, vol. 63, no. 2, pp. 474–482, 2014.
- [10] D. S. Kozlov *et al.*, "Passive intermodulation of analog and digital signals on transmission lines with distributed nonlinearities: Modelling and characterization," *IEEE Transactions on Microwave Theory and Techniques*, vol. 64, no. 5, pp. 1383–1395, 2016.
- [11] J. Henrie, A. Christianson and W. J. Chappell, "Prediction of passive intermodulation from coaxial connectors in microwave networks," *IEEE Transactions on Microwave Theory and Techniques*, vol. 56, no. 1, pp. 209–216, 2008.
- [12] K. M. Gharaibeh, *et al.*, "The Importance of nonlinear order in modeling intermodulation distortion and spectral regrowth," in *Proc. RAWCON 2002. 2002 IEEE Radio and Wireless Conference*, Seattle WA, 2002, pp. 161–164.
- [13] L. Zhang, *et al.*, "A composite exponential model to characterize nonlinearity causing passive intermodulation interference," *IEEE Transactions on Electromagnetic Compatibility*, vol. 61, no. 2, pp. 590–594, 2018.
- [14] L. Zhang, H. Wang, *et al.*, "A Segmented polynomial model to evaluate passive intermodulation products from low-order PIM measurements," *IEEE Microwave and Wireless Components Letters*, vol. 29, no. 1, pp. 14–16, 2018.
- [15] D. S. Kozlov, A. P. Shitvov, and A. G. Schuchinsky, "Characterisation of passive intermodulation in Passive rf devices with X-parameters," in *Proc. Antennas and Propagation Conference*, Loughborough, Leicestershire, United Kingdom, 2014, pp. 64–67.
- [16] D. S. Kozlov, A. P. Shitvov, and A. G. Schuchinsky, "Polynomial model for high-order and multi-carrier passive intermodulation products," in *Proc. 46th European Microwave Conference (EuMC)*, London, 2016, pp. 631–634.
- [17] J. R. Wilkerson, K. G. Gard, and M. B. Steer, "Automated broadband high-dynamic-range nonlinear distortion measurement system," *IEEE Transactions on Microwave Theory and Techniques*, vol. 58, pp. 1273–1282, 2010.
- [18] J. J. Henrie, A. J. Christianson, and W. J. Chappell, "Linear–nonlinear interaction and passive intermodulation distortion," *IEEE Transactions on Microwave Theory and Techniques*, vol. 58, no. 5, pp. 1230–1237, 2010.
- [19] A. M. Saleh, "Intermodulation analysis of FDMA satellite systems employing compensated and uncompensated TWT's," *IEEE Trans. on Communications*, vol. 30, no. 5, 1982.
- [20] G. Macchiarella and A. Sartorio, "Passive Intermodulation in microwave filters: Experimental investigation," in *Proc. IEEE MTT-S Int. Microw. Symp. Dig. WMB-7 Filter II Workshop*, Long Beach, CA, Jun. 2005.
- [21] J. Sombrin, G. S. Pun, and I. Albert, "New models for passive nonlinearities generating intermodulation products with non-integer slopes," in *Proc. 2013 7th European Conference on Antennas and Propagation (EuCAP)*, pp. 25–28, 2013.
- [22] A. Schuck and B. E. J. Bodmann, "Audio nonlinear modeling through hyperbolic tangent functionals," in *Proc. 19th International Conference on Digital Audio Effects (DAFx-16)*, Brno, Czech Republic 2016, pp. 1–6.
- [23] N. J. M. Marques and B. M. D. Brio, "Sensor linearization with neural networks," *IEEE Transactions on Industrial Electronics*, vol. 48, no. 6, pp. 1288–1290, 2001.
- [24] K. M. Gharaibeh, O. A. Zoubi, and A. A. Alzayed, "Adaptive predistortion using threshold decomposition-based piecewise linear modeling," *International Journal of RF and Microwave Computer-Aided Engineering*, vol. 21, no. 2, pp. 145–156, 2011.
- [25] S. Chen, S. A. Billings, and W. Luo, "Orthogonal least squares methods and their application to non-linear system identification," *International Journal of Control*, vol. 50, no. 5, pp. 187–1896, 1989.
- [26] M. Z. Waheed, *et al.*, "Digital self-interference cancellation in inter-band carrier aggregation transceivers: Algorithm and digital implementation perspectives," in *Proc. 2017 IEEE International Workshop on Signal Processing Systems (SiPS)*, pp. 1–5, 2017.
- [27] M. Z. Waheed, *et al.*, "Digital cancellation of passive intermodulation in FDD transceivers," in *Proc. 52nd Asilomar Conference on Signals, Systems, and Computers*, Pacific Grove, CA, 2018, pp. 1375–1381.
- [28] T. I. Lu, *et al.*, "Adaptive Suppression of passive intermodulation in digital satellite transceivers," *Chinese Journal of Aeronautics*, vol. 30, no. 3, pp. 1154–1160, 2017.
- [29] K. Gharaibeh, "Assessment of various window functions in spectral identification of passive intermodulation," *Electronics*, vol. 10, no. 1034, 2021.

Copyright © 2024 by the authors. This is an open access article distributed under the Creative Commons Attribution License ([CC BY-NC-ND 4.0](https://creativecommons.org/licenses/by-nc-nd/4.0/)), which permits use, distribution and reproduction in any medium, provided that the article is properly cited, the use is non-commercial and no modifications or adaptations are made.